Research Article Available online www.ijsrr.org ISSN: 2279–0543

International Journal of Scientific Research and Reviews

Kinetics and Non-Isothermal Decomposition of (*E*)-Methyl -2-hydroxy-5-((3-Nitrophenyl)diazenyl)benzoate (MHNDB) in Air Atmosphere

K Nagendra babu, G. Vallal Perumal, G. Rajarajan, G. Manikandan, V. Thanikachalam*

Department of chemistry, Annamalai University, Annamalainagar -608002. India
DOI - https://doi.org/10.37794/IJSRR.2023.13103

ABSTRACT

(*E*)-Methyl-2-hydroxy-5-((3-nitrophenyl)diazenyl)benzoate(MHNDB) was prepared from diazotisation of m-nitroaniline sodium nitrate with conc. HCl at 0-5oC and coupled with methylsalicylate at pH 8-9. The obtained product was characterized by using microanalysis, FT-IR, ^{1}H and ^{13}C NMR, and mass spectral techniques. Thermal decomposition curves (TG, DTA, and DTG) at different heating rates were recorded for MHNDB in the air atmosphere. TG curves show that MHNDB was decomposed in a single step with an A2 decomposition mechanism. Friedman, KAS, and FWO methods determined the energy of activation and frequency factor. The invariant kinetic parameters coincided with values obtained by the Friedman and FWO methods. Thermodynamic parameters were also investigated.

KEYWORDS: Non-isothermal, Master plot, Friedman, Flynn-Wall-Ozawa, Kissinger, Akahira, Sunose, invariant kinetic parameters.

***Corresponding author**

Dr.V. Thanikachalam

Department of Chemistry,
Annamalai University,
Annmalainagar-608002, INDIA.
Email: pvta1998@yahoo.co.in, Mob No. – 9488476098

INTRODUCTION

Methylsalicylate is a physiological and biochemical process regulator. It is produced by plants, which also contribute to the synthesis of lignin, which is resistant to disease, abiotic stress, and allelopathic stress.[1-4] The volatile substance methylsalicylate, which confers resistance in plants, is derived from salicylic acid. It is also a helpful tool for treating ailments.[5-8] Kalaivani et al.[9]investigated for enhancing methylsalicylate activity in the rice seed sector to encourage development and output. Methylsalicylate was added in smaller amounts to mints, ice cream, and perfumes, whereas larger doses were a rubefacient and analgesic for muscle and joint pain. Nowadays, methylsalicylate is widely used in the atmosphere and is necessary for its detection and decrease. Anti-inflammatory solid effects are exhibited by methyl salicylate compounds, including piperazine.[10] In traditional Chinese medicine, methyl salicylate glycosides are a typical therapy for rheumatoid arthritis.[11]They are studied for potential utility in treating a variety of ailments in both humans and plants due to their pharmacological qualities.[12]

Azo compounds are widely used as colorants in consumer products such as food coloring, textiles, printing, cosmetics, and pharmaceuticals. Currently, about 3000 azo dyes are in use throughout the world. It is separated into four groups: dyes that are monoazo, diazo, triazo, and polyazo. But most of them are monoazo compounds, which join two aromatic systems structurally through the azo chromophore and another use is in analytical chemistry.[13]
On the other hand, azo compounds have demonstrated biological activities that include antioxidants, polymeric biodegradable prodrugs, antibacterial properties,[14,-17] and medicinal uses, as well as the suppression of both Gram-positive and Gram-negative bacteria in solvents like DMSO and DMF.[18,19]Anions play a significant role in our daily lives since they are necessary for numerous industrial activities and physiological processes.[20]Much work has been reported on designing novel anionic species transporters, sensors, and receptors[21]. Most chemosensors developed to date are chromogenic and fluorescent sensors, which change dramatically in their photophysical properties in the presence of anions.[22] Creating colorimetric anion sensors is one topic of great interest in this context.[23] With these sensors, anions can be found using only the human eye and no spectroscopic equipment.[24] In recent years, chromogenic sensors for cations,[25] have been created. Azo-based colorimetric sensors for anions have been the subject of several reports.[26-28]Nagendra Babu et al[29]reported the thermalvaporization of (*E*)-methyl-2-hydroxy-5-(phenyldiazenyl)benzoate under non-isothermal conditions in air atmosphere.No reports are available on thermal decomposition of ((*E*)-methyl-2-

hydroxy-5-((3-nitrophenyldiazenyl)benzoate(MHPDB) under the non-isothermal conditions in the air atmosphere.

EXPERIMENTAL

Materials and Methods

m-Nitroaniline, methylsalicylate, sodium nitrite, Conc.HCl and sodium hydroxide were used as purchased from analaR grade of SD-fine chemical Ltd, India.

At Teena laboratories limited, industrial estate, Hyderabad, India, the mass confirmation analysis was completed for test methodologies, specifically DIP-MS by Liquid Chromatograph-mass spectrometer (LC-MS). A Fourier transform infrared spectrophotometer (FT-IR) was used with Bruker alpha apparatus and software to perform the fingerprint of the MHNDB confirmation study, prepared using the KBr pellet method and scanned by 16 scans at a resolution of $2cm^{-1}$ between the frequency range of 4000-650 cm^{-1}.^{1}H (400 MHz) and ^{13}CNMR (100 MHz) spectra were recorded at Agilent-SA equipped with software, Hyderabad, India. The thermal analysis was carried out using a Thermogravimetry and Differential thermal analyzer, Simultaneous Thermal Analyzer, STA 7200, Hitachi HTG, Japan, at Vignan University, Guntur, Andhra Pradesh. TG, DTG and DTA analyses in a ceramic crucible under a static air atmosphere (100 mL min^{-1}) with a sample mass of about 8 mg and heating rates of 5, 10, and 15 K min^{-1} from 23 to 700^{o}C. The sample temperature, which is controlled by a thermocouple, did not show any consistent departure from the predetermined linear temperature program. Equipped software was used to calculate the kinetic parameters E_a and ln A.

Synthesis of ((E)-methyl-2-hydroxy-5-((3-nitrophenyl)diazenyl)benzoate(MHNDB)

m-Nitroaniline was used as the starting material for the synthesis of the azo compound,[29] which was diazotisation with a cold solution of sodium nitrite and concentrated hydrochloric acid, followed by an aqueous sodium hydroxide (10%) solution of methylsalicylate. A brownish substance was isolated, filtered out, washed with aqueous methanol, and then recrystallized with ethanol. This was characterised by GC mass m/z 123, FT-IR(cm^{-1}), 3210 υ (O-H),2952 υ(C-H), 1678 υ(C=O), 1439υ(C=C), 1159 υ(N=N), 1070 υ(C-O) and 836 υ(C-H).^{1}H-NMR (400 MHz, DMSO-d_6) δ 10.992 (1 H), 8.300 -8.293(d, 1H), 8.089-8.062 (dd,3H), 7.880-7.862(d,2H), 7.632-7.532 (3H), 7.204-7.181 (1H), 3.986-3.942 (3H). ^{13}C-NMR (100 MHz, DMSO-d_6) δ168.24 (ester carbonyl), 162.16 (C-O), 151.75 (C-N), 144.42 (C-N), 131.08, 129.32, 128.72, 125.54, 122.35,118.50,113.96 (aromatic carbons)

and 52.61 (O-CH_3).

Model-free iso-conversional methods

m_i, m_t, m_α, are represented as initial mass, mass at a particular temperature, and final mass of sample, respectively. The degree of conversion can be determined from the below equation.

$$\alpha = \frac{m_i - m_t}{m_i - m_\alpha}$$

Friedman's method

Friedman's [30] model-free (iso-conversational) kinetic analysis method is used to determine the impact of activation energy E_α on the degree of conversion(α). From the linear plot of ln [β dα/dT] versus 1/T, the activation energy and a frequency factor are obtained from the slope and intercept.

$$ln\left[\beta\frac{d\alpha}{dT}\right] = ln[A_\alpha f(\alpha)] - \frac{E_{a,\alpha}}{RT_\alpha} \quad \text{.....(1)}$$

Flynn-Wall-Ozawa (FWO) method

The FWO[31] procedure is a model-free method that entails plotting ln(β) versus 1/T, determining E_a from the slopes of such plots, and measuring the temperatures corresponding to fixed values of degree of conversion (α) from experiments at different heating rates, β.

$$ln\,\beta = ln\left[\frac{0.0048\,AE_a}{g(\alpha)\,R}\right] - 1.0516\frac{E_a}{RT} \quad \text{.....(2)}$$

Method of Kissinger, Ahira, and Sunose (KAS)

The KAS [32]is a model-free, isoconversional kinetic analysis method that establishes the connection between activation energy E_a and degree of conversion α for dynamic studies at various constant heating rates β. The plotting of ln (β/T^2) versus 1/T reveals the slope and intercept of the linear plot, from which the activation energy and the frequency factor, can be determined.

$$\ln\left(\frac{\beta}{T^2}\right) = ln\left[\frac{AE_a}{g(\alpha)\,R}\right] - \frac{E_a}{RT} \quad \text{.....(3)}$$

Model-fitting method

Coats and Redfern

Model fitting—kinetic parameters were computed using approximately fifteen models—was used in the Coats and Redfern [33] algorithm. Out of the fifteen models, one is the best linearity. A

linear plot of ln [(g(α))/T^2] versus 1/T yields the pre-exponential values and the activation energy from the intercept and slope, respectively.

$$\ln\left[\frac{g(\alpha)}{T^2}\right] = ln\left(\frac{AR}{\beta E_a}\left[1-\left(\frac{2RT^*}{E_a}\right)\right]\right) - \frac{E_a}{RT} \ldots\ldots(4)$$

Kissinger equation for peak temperature [34]

$$\ln\left(\frac{\beta}{T_m^2}\right) = -\frac{E_a}{RT_m} + \ln\left(\frac{AR}{E_a}\right) \qquad \ldots\ldots(5)$$

The frequency factors and thermodynamic parameters are estimated from the following equations: [35-40]

$$A = \frac{ex k_B T_P}{h} \exp\left(\frac{\Delta S^{\#}}{R}\right) \ldots\ldots. (6)$$

$$\Delta S^{\neq} = R \ln \frac{Ah}{e\chi k_B T_p} \ldots\ldots. (7)$$

Since $\Delta H^{\neq} = E_a - RT_p$ ..... (8)

$$\Delta G^{\neq} = \Delta H^{\neq} - T_p \Delta S^{\neq} \ldots\ldots. (9)$$

Where R (R= 8.314 $JK^{-1}mol^{-1}$) is the gas constant, h (h = $6.626x10^{-34}$ J sec^{-1}) is the Planck constant, k_B(k_B= $1.38x10^{-23}JK^{-1}$) is the Boltzman constant, T_p is the peak temperature of the DTG curve and A, $\Delta H^{\#}$, $\Delta S^{\#}$, $\Delta G^{\#}$ are the frequency factors (A), enthalpy($\Delta H^{\#}$), entropy($\Delta S^{\#}$) and free energy of activation ($\Delta G^{\#}$), respectively.

RESULTS AND DISCUSSION

The decomposition of the MHNDB takes place in a single stage, as shown in the TG curves at different heating rates of 5, 10, and 15 K min^{-1} (**Fig. 1**). According to TG curves, **MHNDB** begins to melt at 162.5°C and decompose around 200°C. The peak of the curves corresponds to the weight loss shown in the TG curves while heating **MHNDB** from room temperature to 200°C and ending at 320°C. As the heating rate increases, the maximum temperature shifts to higher temperatures in all of the asymmetric thermogravimetric curves.

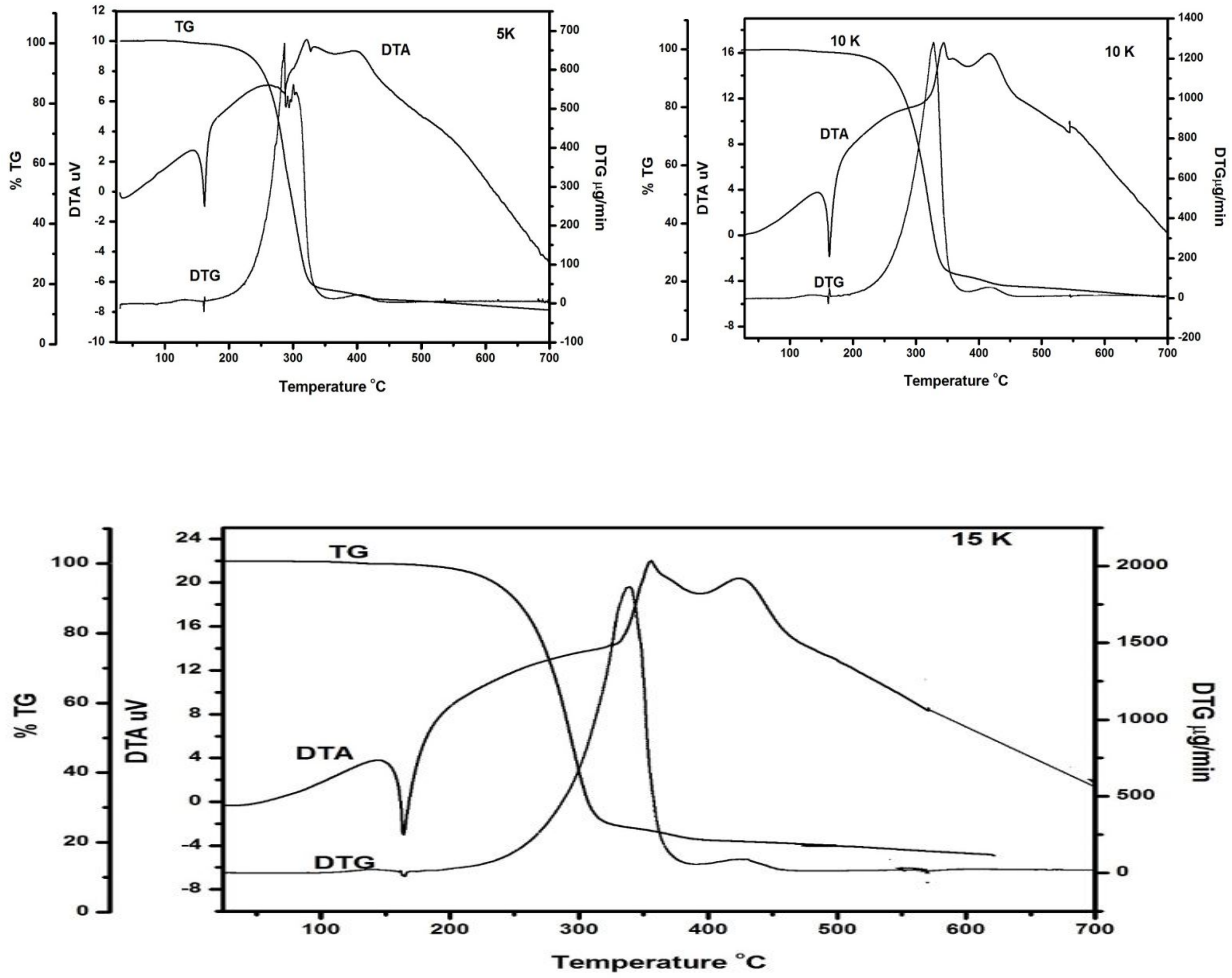

Fig.1.Thermal decomposition of MHNDB at the heating rates 5, 10 and 15K m^{-1} under non-isothermal conditions.

Model-free analysis

The thermal behaviour of MHNDB was initially examined under non-isothermal decomposition using model-free methods such as Friedman,[30] Flynn-Wall-Ozawa,[31]and Kissinger-Akahira-Sunose[32].The data illustrate how the apparent activation energy (E_a) for MNHDB varies with the degree of conversion (α). In the conversion range of $0.20 \leq \alpha \leq 0.90$, the E_a value decreases somewhat and increases with the degree of conversion (Table 1). The Friedman and FWO isoconversional methods that obtained the E_a values are close to each other. Furthermore, the data show that the apparent activation energy (E_a) is dependent on the extent of conversion (α), which aids in revealing the intricate nature of the decomposition process as well as identifying the mechanism of decomposition.

According to the Friedman method, the average decomposition activation energy (E_a) is 63.96 ± 1.14 kJ mol^{-1} (0.10 ≤α ≤ 0.90). It is clear that the activation energies calculated using the Friedman approach are somewhat close to those computed using the FWO method and more in line with the KAS method. The activation energy is slightly variable in the 0.10 ≤α ≤ 0.90 range regardless of the calculation method employed using the Friedman, KAS, and FWO methods, with average values of E_a = 63.96 ± 1.14, 57.41 ± 1.65, and 75.49 ± 1.04 kJ mol^{-1}, respectively.

Table1. Temperatures corresponding to the same degree of conversion at different heating rates for MHNDB

α	Temperature (K)			Friedman method		KAS method		FWO method	
	5 (K min^{-1})	10 (K min^{-1})	15 (K min^{-1})	E_a (kJ mol^{-1})	r	E_a (kJ mol^{-1})	r	E_a (kJ mol^{-1})	r
0.05	501.47	514.60	528.26			81.81	-0.987	85.93	-0.989
0.1	521.08	535.50	550.86	76.64	-0.983	64.50	-0.989	83.69	-0.988
0.15	531.63	547.40	563.87	68.77	-0.987	61.77	-0.990	80.81	-0.989
0.2	539.00	556.10	573.07	66.22	-0.995	59.98	-0.992	78.95	-0.992
0.25	544.63	562.40	580.17	64.27	-0.985	58.52	-0.992	77.41	-0.991
0.3	549.38	567.35	585.92	66.62	-0.972	57.75	-0.990	76.61	-0.990
0.35	553.25	572.07	590.90	61.20	-0.997	56.78	-0.992	75.61	-0.991
0.4	556.57	575.50	595.21	59.86	-0.951	55.81	-0.990	74.55	-0.990
0.45	559.59	579.14	599.10	59.73	-0.995	55.12	-0.991	73.84	-0.991
0.5	562.23	582.67	602.51	58.83	-0.999	54.58	-0.993	73.30	-0.993
0.55	564.90	586.21	605.70	63.88	-0.994	54.41	-0.995	73.19	-0.995
0.6	567.53	589.46	608.80	64.88	-0.999	54.27	-0.996	73.10	-0.996
0.65	570.20	593.12	611.95	63.93	-0.983	54.11	-0.998	73.01	-0.997
0.7	572.80	596.38	615.05	63.52	-0.997	53.89	-0.999	72.83	-0.998
0.75	575.80	600.05	618.54	65.15	-0.997	53.75	-0.999	72.75	-0.999
0.8	579.10	604.00	622.48	63.39	-0.999	53.48	-1.000	72.52	-0.999
0.85	584.20	609.18	628.46	65.77	-0.988	53.33	-0.999	72.43	-0.998
0.9	603.00	626.40	652.85	54.69	-0.889	49.62	-0.985	68.45	-0.987
			Avg	63.96 ± 1.14		57.41 ± 1.65		75.49 ± 1.04	

Model-fitting analysis

Then, each of the 15 models[33]given in Table 2 was fitted with the non-isothermal kinetic data of MHNDB at 0.10 ≤ α ≤ 0.90, where model-free analysis indicated essentially constant activation energy. The reaction model that is selected has a significant influence on the values of the activation energy (E_a), pre-exponential factor (ln A), coefficient of linear correlation (r), and kinetic models that describe the decomposition process. The invariant kinetic parameters technique supports the result drawn based on the kinetic data, demonstrating that the decomposition occurred with a single mechanism.

Table 2. Determination ofapparent activation parameters by Coats-Redfern method for each heating rate MHNDB

Kinetic models	β = 5 K min^{-1}			β = 10 K min^{-1}			β = 15 K min^{-1}		
	E_a (kJ mol^{-1})	ln A (A min^{-1})	r	E_a (kJ mol^{-1})	ln A (A min^{-1})	r	E_a (kJ mol^{-1})	ln A (A min^{-1})	r
P2	28.78	2.83	-0.970	27.96	3.06	-0.963	27.11	3.02	-0.951
P3	16.06	-0.34	-0.957	15.41	0.01	-0.946	14.74	0.07	-0.927
P4	9.74	-2.12	-0.934	9.17	-1.73	-0.917	8.59	-1.63	-0.884
F1	97.18	18.64	-0.998	95.34	18.20	-0.993	93.56	17.55	-0.985
F2	139.32	28.49	-0.994	136.92	27.65	-0.990	134.67	26.64	-0.984
F3	191.51	40.53	-0.981	188.45	39.20	-0.978	185.67	37.74	-0.972
D1	143.04	27.60	-0.981	140.64	26.74	-0.977	138.22	25.66	-0.970
D2	159.72	30.81	-0.988	157.02	29.78	-0.984	154.35	28.54	-0.977
D3	180.88	34.23	-0.995	177.85	32.98	-0.990	174.81	31.52	-0.983
D4	166.69	30.93	-0.991	163.88	29.83	-0.987	168.44	29.94	-0.977
A2	43.94	6.68	-0.997	42.87	6.77	-0.991	41.82	6.59	-0.981
A3	26.16	2.44	-0.996	25.34	2.69	-0.989	24.33	2.62	-0.976
A4	17.32	0.17	-0.995	16.63	0.50	-0.985	15.95	0.56	-0.968
R2	80.58	14.00	-0.991	79.00	13.73	-0.986	77.43	13.22	-0.978
R3	75.89	13.16	-0.987	74.38	12.94	-0.983	72.88	12.47	-0.974

Invariant kinetic models

The invariant kinetic parameters was employed to obtain data for heating rates of 5, 10, and 15 K min^{-1}. The kinetic parameters are evaluated using the Coats-Redfern method (Table 2). For these kinetic models, the straight lines corresponding to the Coats-Redfern[33]examination are shown by correlation coefficient values that are close to unity in the range $0.10 \leq \alpha \leq 0.90$. Table 3 demonstrates that the values of $E_{a\ and}$ ln A are influenced by the heating rate and the kinetic model. The pre-exponential factor and actual activation energy, which are also referred to as the invariant kinetic parameters, are computed simply by plotting ln A_{inv} vs. E_{inv} for a number of constant heating rates. The resultant straight lines should intersect at a specific point (E_{inv}, A_{inv}).[42-44]

The evaluation of the invariant kinetic parameters is performed using the supercorrelation equation. The plot of a_β*versus* b_β, obtained for three constant heating rates, is a straight line whose parameters allow the determination of ln A_{inv} and E_{inv}.[42-44]Erofe'vmodel among all other models, although its apparent parameters were obtained with high correlation coefficients (Table 4).

Table 3. Compensation effect parameters for several combinations of kinetic models for MHNDB

β ($K\ min^{-1}$)	AKM			AKM–{P4,F1,F2,F3,D1,D2,A2, A3,A4,R2,R3}		
	a_β ($A\ min^{-1}$)	b_β (mol J^{-1})	r	a_β ($A\ min^{-1}$)	b_β (mol J^{-1})	r
5	-3.50538	0.21835	0.9972	-3.81262	0.22586	0.9985
10	-2.91191	0.21174	0.9969	-3.21564	0.21935	0.9983
15	-2.58618	0.20509	0.9966	-2.91396	0.21321	0.9982
β ($K\ min^{-1}$)	AKM-{F1,F2,F3,A2,A3,A4,R2,R3}			AKM-{P2, F1,F2,F3, A3,A4,R3}		
	a_β ($A\ min^{-1}$)	b_β (mol J^{-1})	r	a_β (A min^{-1})	b_β (mol J^{-1})	r
5	-3.88898	0.23102	0.9995	-3.87019	0.23145	0.9998
10	-3.2817	0.22451	0.9995	-3.35726	0.22497	0.9998
15	-2.96869	0.21838	0.9995	-2.95292	0.21883	0.9998

Table 4. IKP for several combinations of kinetic models for MHNDB

Kinetic model	E_{inv}(kJ mol^{-1})	ln A_{inv} ($A\ min^{-1}$)	-r
AKM	69.30 ± 11	11.67 ± 2.5	0.9859
AKM–{P4,F1,F2,F3,D1,D2,A2, A3,A4,R2,R3}	71.25 ± 12	12.32 ± 2.7	0.9855
AKM-{F1,F2,F3,A2,A3,A4,R2,R3}	73.02 ± 12.2	13.02 ± 2.73	0.9864
AKM-{P2, F1,F2,F3, A3,A4,R3}	72.74± 3.84	12.98 ± 0.86	0.9986

Determination of the kinetic model by master plots

The integral function of conversion in the solid state nonisothermal decomposition[46]reactions is expressed as

$$g(\alpha) = \left(\frac{A}{\beta}\right) \int_{T_0}^{T} \left(\frac{-E}{RT}\right) dT = \left(\frac{AE}{\beta R}\right) p(u) \quad \ldots\ldots(10)$$

where $p(u) = \int_{\infty}^{u} \left(-\frac{e^{-u}}{u^2}\right) du$ and u = E/RT.

Using a reference at point α =0.5, and according to FWO method one gets

$g(\alpha_{0.5}) = (\frac{AE}{\beta R}) p(u_{0.5})$ ……(11)

where $u_{0.5} = E/RT_{0.5}$when equation (11) is divided by (12) the following equation is obtained

$$\frac{g(\alpha)}{g(\alpha_{0.5})} = \frac{p(u)}{p(u_{0.5})} \quad \text{……(12)}$$

Plots of $g(\alpha)/g(\alpha_{0.5})$ against α match the master plots of other hypothetical g(∞) functions that are provided in Table 4. An estimated formula[46] of p(u) with good precision is used to build the experimental master plots of p(u)/p(u0.5) against, using experimental data gained under different heating rates: p(u) = exp(−u)/[u(1.00198882u + 1.87391198)]. When the appropriate kinetic model is utilized, Eq. (12) indicates the experimental values of $g(\alpha)/g(\alpha_{0.5})$ are comparable for a given α. The kinetic model can be established via comparison of the theoretical and experimental master plots**(Fig.2)**.

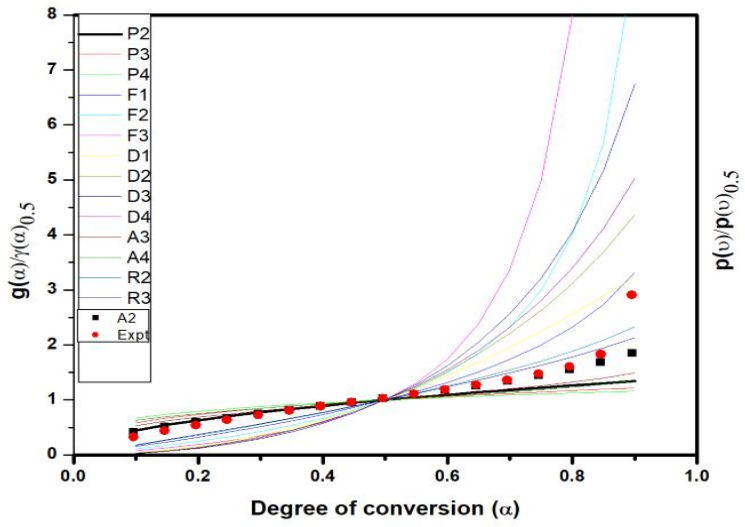

Fig. 2. Plot of g(α)/g(α0.5) and p(u)/p(u0.5) versus degree of conversition.

By comparing the experimental master plots with the theoretical ones[47-49] we can determine the kinetic model related to the thermal decomposition of **MHNDB**. To confirm the thermal decomposition mechanisms of **MHNDB**, the theoretical master plots of various kinetic functions against α were constructed from experimental data for the thermal decomposition stages of**MHNDB** under different heating rates in air atmosphere. The comparisons of the experimental and theoretical master curves show that the thermal decomposition of **MHNDB** agrees with the A2 master curve for the decomposition stage. The pre-exponential factor can be obtained from the intercepts of the regression lines

corresponding to various heating rates.A similar type of decomposition mechanism was reported by Nagendra Babu et al[29]for thevaporization of (*E*)-methyl-2-hydroxy-5- (phenyldiazenyl) benzoate under non-isothermal conditions in the air. By assuming the theoretical A2 laws, the logarithmic value of the pre-exponential factor (ln A) obtained from the correlation coefficient of the plots of $\ln[1-(1-\alpha)^{1/2}]$ versus $E_a p(u)/\beta R$ for the decomposition stage is found to be $13 \pm 0.15\ s^{-1}$(Fig 3).

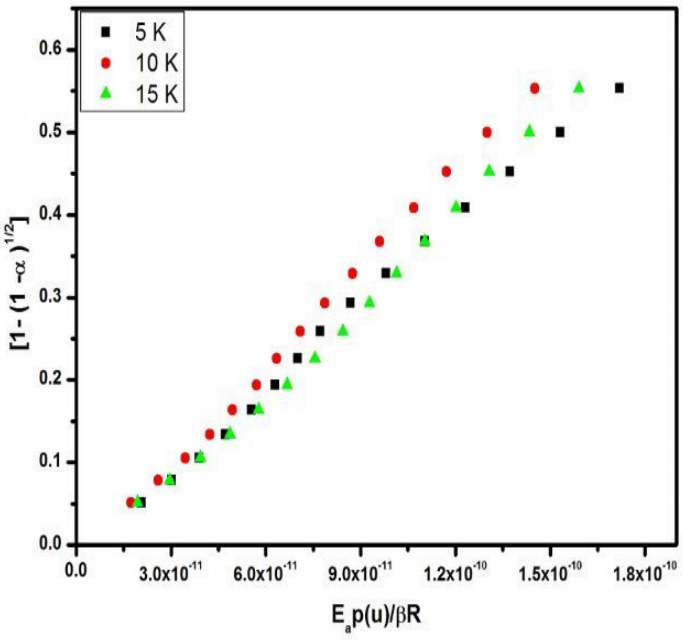

Fig. 3. Plot of $E_a p(u)/\beta R$ versus $[1-(1-\alpha)^{1/2}]$ for MHNDB

Thermodynamic parameters

Thermodynamic data were determined using equations (6-9)[36-41] for MHNDB and values are displayed in Table 5. The negative value of entropy, the free energy value is positive, which reveals that the decomposition process is endothermic in nature due to the absorption of heat during the decomposition process of the studied compound.

Table 5. Thermodynamic parameters of MHNDB under non-isothermal condition (DTG peak temperature)

Heating rate ^oK	Temp ^oK	lnA (min^{-1})	E_akJ/mol	ΔS J/Kmol	ΔH kJ/mol	ΔG kJ/mol
5	575.70			-144.60	70.48	153.74
10	601.00	13.72	75.27 ± 5.71	-144.96	70.27	157.40
15	613.00			-145.13	70.18	159.24

CONCLUSION

The studied compound decomposed in a single stage with the absorption of heat. The model for the decomposition mechanism is A2(Avrami-Erote'v Model). The thermal stability is less and the energy of activism by model-free methods coincided almost with E_a by thermodynamic parameters. The entropy valve is negative, which indicates that the compound decomposed to a higher state. Free energy is positive, which indicates that the absorption of heat and decomposition in non-spontaneous processes and confirmed TG-DTG/DTA curves.

Acknowledgement

One of the authors (N K) acknowledged Teena laboratories limited, Telangana, for mass and FT-IR, Agilent -SA equipped with software, Prashanthi Nagar, Hyderabad, for ^{1}H(400 MHz) and ^{13} CNMR (100 MHz), Simultaneous thermal analyzer, STA 7200, Hitachi HTG, Andhra Pradesh, for TG, DTA and DTG analyses.

Conflict of interest

We declare that we do not have any conflict of interest

REFERENCES

1. Raskin. I. Role of salicylic acid in plants. *Ann. Rev. Plant Biol*. 1992; 43: 439–463.
2. Humphreys J. M. and Chapple, C. Rewriting the lignin roadmap. *Curr. Opi. Plant Biol*; 2002; 5: 224–229.
3. YusufM. Hayat, S. Alyemeni, M. N. Fariduddin, Q. and Ahmad, A. Salicylic Acid Physiological Roles in Plants.*Springer*2013; 15–30.
4. Wiesel L. DavisJ. Milne L. A transcriptional reference map of defence hormone responses in potato. *Sci, Rep.* 2015; 15229:1-12.
5. VazirimehrM. Rigi K.and Branch Z. Effect of salicylic acid in agriculture. *Int. J. Plant Anim. Environ. Sci.*2014; 4: 291–296.
6. TavaresL. C. Rufno, C. A. Oliveira S. d. Brunes A. P. and Villela F. A. Treatment of rice seeds with salicylic acid: seed physiological quality and yield. *J. Seed Sci.* 2014; 36: 352–356.
7. TangF. Fu Y.-Y. and YeJ.-R. Te effect of methyl salicylate on the induction of direct and indirect plant defense mechanisms in poplar (Populus× euramericana'Nanlin 895'). *J. Plant Inter.* 2015; 10: 93–100.

8. Kauffman H. Reddy A. Hsieh, S. andMerca S. Improved technique for evaluating resistance of rice varieties to Xanthomonas oryzae.*Plant Dis. Rep.* 1973;57(6):537-541.
9. Kandaswamy Kalaivani, Marimuthu Maruthi Kalaiselvi andSengottayan Senthil Nathan, Effect of methyl salicylate (MeSA), An elicitor on growth, physiology and pathology of resistant andsusceptible rice varieties*Sci Rep.* 2016; 34498.https://doi.org/10.1038/srep34498.
10. Jingfen Li, LishengWang ,Pengyun Liang ,Menghua Li,Xu Liu ,Lichuan Wu, and Hua Yang , Synthesis, Characterization, and Anti-Inflammatory Activities of Methyl Salicylate Derivatives Bearing Piperazine Moiety. *Molecules,* 2016, 21(11), 1544,https://doi.org/10.3390/molecules21111544.
11. Ying Dong, Xiao Li, Yicheng Zhao ,Xueyang Ren , Yuan Zheng , Ruolan Song , Xiangjian Zhong ,Dongjie Shan , Fang Lv , Qingyue Deng , Xianxian Li , Yingyu He , Keyan Chai , Xiuhuan Wang, Gaimei She, Biotransformation and metabolism of three methyl salicylate glycosides by gut microbiota in vitro.*J. Pharm. Biomed. Anal.*2023; 233:115474. https://doi.org/10.1016/j.jpba.2023.115474.
12. Rosheen, Shivali Sharma and Divya Utreja, Salicylic Acid: Synthetic Strategies and Their Biological Activities.*ChemistrySelect*, 2023; 8(13).https://doi.org/10.1002/slct.202204614.
13. Anderson R.G. and Nickless G. Heterocyclic azo dyestuffs in analytical chemistryA review,*Analyst*,1967; 92: 207-238.https://doi.org/10.1039/AN9679200207.
14. GargH.G.and SharmaR.A., Potential antineoplastics. I. 2-Amino-4,6-dimethyl-5-arylazopyrimidines and 1-thiocarbamoyl-3,5-diphenyl-4-arylazopyrazoles.*J. Med. Chem.*1996; 12: 1122-1124.https://doi.org/10.1021/jm00306a047
15. Ali L and Adnan S.Synthesis and Characterization of New Diazo Derivatives, and Study of their Biological Activity. *Int. J. Drug Deliv. Technol.*2022;12(1):231-236.
16. Loganathan K.Sithick A. Purushothaman, Silambarasan Sand Jamal A. Synthesis and characterization of Azo derivatives of diacetylresorcinol. *J. Chem. Pharm. Res.* 2015;7:1452-1455.
17. Sabrean F. J. Shaimaa A. Mohammad and N Al-baiati, Flammability of Polyester and Epoxy Resins by Using Some of a New Organic Compounds. *Int. J. Psychosoc. Rehabilitation.* 2020;24:1375-1394.
18. Chandrashekhar J. Patil and Chandrakant A. Nehete, The Azo Derivatives of Salicylic Acid. *Int. J. Pharm. Sci. Rev. Res.* 2015; 33(2):248-256.

19. Shipra Baluja and Sumitra Chanda, Synthesis And Screening Of Some Azomethines Bearing Methyl Salicylate Moiety For Antibacterial Activities. *Indonesian J. Pharm.,*2016;27(2):92-98.https://doi.org/10.14499/INDONESIANJPHARM27ISS2PP92.
20. DukeR.M. VealeE.B. PfefferF.M. KrugerP.E. Gunnlaugsson T. Colorimetric and fluorescent anion sensors: an overview of recent developments in the use of 1,8-naphthalimide-based chemosensors,*Chem. Soc*. 2010; 39: 3936-3953. https://doi.org/10.1039/B910560N.
21. CaltagironeC.and GaleP.A. Anion receptor chemistry: highlights from 2007.*Chem. Soc.* 2009; 38: 520-563.https://doi.org/10.1039/B806422A.
22. Shuzhen Hu, Yong Guo Jian Xu andShijun Shao, A selective chromogenic molecular sensor for acetate anions in a mixed acetonitrile–water medium,*Org*. *Biomol. Chem*. 2008; 6: 2071-2075, https://doi.org/10.1039/B805291C.
23. Chuan-Feng Chen and Qi-Yin Chen, Azocalix[4]arene-based chromogenic anion probes, *New J. Chem*. 2006; 30:143-147, https://doi.org/10.1039/B513355F.

24. Piatek P. Jurczak. A selective colorimetric anion sensor based on an amide group containing macrocycle, *Chem. Commun*. 2002; 20:2450-2051,https://doi.org/10.1039/B207335H.
25. Dengqing Zhang and Wusong Jin, Highly selective and sensitive colorimetric probe for hydrogen sulfide by a copper (II) complex of azo-dye based on chemosensing ensemble approach. *Spectrochim. Acta Part A: Molecular and Biomolecular Spectroscopy.*2012; 90: 35-39.
26. EzaeianK. and Khanmohammadi H. Naked-eye detection of biologically important anions by a new chromogenic azo-azomethine sensor, *Spectrochim.Acta*Part A. 2014; 133: 31-37, https://doi.org/10.1016/j.saa.2014.05.049.
27. Khanmohammadi H., Rezaeian K. andAbdollahi A. Colorimetric detection of anions in aqueous media using N-monosubstituted diaminomaleonitrile-based azo-azomethine receptors: Real-life applications.*Spectrochim. Acta* A. 2015; 139: 405-412,https://doi.org/10.1016/j.saa.2014.12.088.
28. ReenaV. SuganyaS.and VelmathiS.Synthesisand anion binding studies of azo-Schiff bases: Selective colorimetric fluoride and acetate ion sensors. *J. Fluor. Chem*. 2013; 153: 89-95https://doi.org/10.1016/j.jfluchem.2013.05.010.
29. Nagendra Babu K.,Vallal Perumal G., RajarajanG.Manikandan G. and ThanikachalamV., Thermal Vaporization Of (*E*)-Methyl-2-Hydroxy-5-(Phenyldiazenyl)benzoate Under Non-Isothermal Condition in Air Atmosphere. *GravidaReviewJ.* 2023; 9(11): 550-573.
30. FriedmanH.L.Kinetics of thermal degradation of char-forming plastics from thermogravimetry. Application to a phenolic plastic*J. Polym. Sci. C: Pol. Lett.,*1963; 6: 183-195.
31. Flynn J.H. and WallL.A. General Treatment of the Thermogravimetry of Polymers. *J. Res. Natl. Bur. Stand.* A, 1966; 70: 487-523. T.Ozawa , A New Method of Analyzing Thermogravimetric Data.*Bull.Chem. Soc. Jpn*., 1965; 38: 1881–6.
32. AkahiraT. and SunoseT.Joint Convention of Four Electrical Institutes.*Res.Rep.Chiba. Inst. Technol.,* 1971; 16: 22-31.
33. CoatsA.W. and J.P. Redfern, Kinetic Parameters from Thermogravimetric Data.*Nature*,1964;201: 68–69, https://doi.org/10.1038/201068a0.
34. Kissinger H.E. Reaction Kinetics in Differential Thermal Analysis. *Analytical Chemistry,*1957; 29: 1702-1706.
35. Sestak J. Thermodynamical properties of solids, *Academia Prague*, 1984.
36. BamfordC.H. and TipperC.F.H. (Eds.), Comprehensive chemical kinetics, reactions in the solid state, 1980; 22: 1-300.

37. CordesH.F.Preexponential factors for solid-state thermal decomposition.*J. Phys. Chem.,*1968; 72(6): 2185-2189.
38. CriadoJ.M., Pérez-MaquedaL.A. andSánchez-JiménezP.E., Dependence of the preexponential factor on temperature.*J. Therm. Anal. Calorim*., 2005; 82: 671-675.
39. SokolskiiD.V. andDruz V.A.Introduction in theory heterogeneous catalysis, VyshayaShkola, Moscow, 1981.
40. VlaevL., NedelchevN.GyurovaK. andZagorchevaM.A comparative study of non-isothermal kinetics of decomposition of calcium oxalate monohydrate.*J. Anal. Appl. Pyrol.,*2008; 81: 253.
41. CriadoJ.M. and MoralesJ.Defects of thermogravimetric analysis for discerning between first order reactions and those taking place through the Avrami-Erofeev's mechanism, *Thermochim. Acta*, 1976; 16:382-387.
42. LesnikovichA.I. and LevchikS.V.A method of finding invariant values of kinetic parameters. *J. Therm. Anal.,*1983; 27: 89-93.
43. LesnikovichA.I. and LevchikS.V.Isoparametric Kinetic relations for chemical transformations in condensed substances (analytical survey).*J. Therm. Anal*. 1985; 30: 237-262.
44. VyazovkinS. and LesnikovichA.I.Estimation of the pre-exponential factor in the isoconversional calculation of effective kinetic parameters.*Thermochim. Acta,*1988; 128: 297-300.
45. BudrugeacP. andSegalE.Applicability of the Kissinger equation in thermal analysis.*J.Therm. Anal. Calorim.,*2007; 88: 703-707.
46. Cai J. and LiL.S. Kinetic analysis of wheat straw pyrolysis using isoconversional methods. *J. Therm. Anal. Calorim*., 2009; 98: 325-330.
47. MãlekJ.The Kinetic Analysis of Non-Isothermal Data.*Thermochim. Acta*, 1992; 200: 257-269.
48. SbirrazzuoliN.,VecchioS. andCatalaniA.,Isoconversional kinetic study of alachlor and metolachlor vaporization by thermal analysis. *Int. J. Chem. Kinet*., 2005; 37: 74.
49. CriadoJ.MalekJ.OrtegaA.Applicability of the master plots in kinetic analysis of non-isothermal data.*Thermochim. Acta*1989; 147: 377–385.